Solar Sail Attitude Control Using Shape Modulation: The Cable-Actuated Bio-inspired Lightweight Elastic Solar Sail (CABLESSail) Concept

Ryan J. Caverly,[a,*], Keegan R. Bunker[a], Nathan Raab[b], Vinh L. Nguyen[a], Garvin Saner[a], Zixin Chen[a], Tyler Douvier[a], Richard J. Lyman[a], Owen Sorby[a], Benjamin Sorge[a], Ebise Teshale[a], Benjamin Toriseva[a]

[a]*Department of Aerospace Engineering and Mechanics, University of Minnesota, Minneapolis, USA*
[b]*Minnesota Robotics Institute, University of Minnesota, Minneapolis, USA*

Abstract

This paper presents the Cable-Actuated Bio-inspired Lightweight Elastic Solar Sail (CABLESSail) concept that will enable robust, precise, and scalable attitude control of solar sails. This concept leverages lightweight cable-driven actuation to achieve large, controllable elastic bending and torsional deformations in the booms of a solar sail that mimic the motion of an elephant's trunk or a starfish's arms. These large cable-driven boom deformations modulate the shape of the entire sail to create an imbalance of SRP to induce control torques in all three solar sail axes. This actuation method scales well with an increase in solar sail size, as cables can transmit forces over kilometers in length from a lightweight and small stowed volume. This paper highlights early work on the CABLESSail concept, focusing on initial research efforts on its design, analysis, modeling, and prototyping.

Keywords: Attitude control, momentum management, flexible structures, cable-driven robots, solar sail design

1. Introduction

Through the use of solar radiation pressure (SRP)-based propulsion, solar sails offer unique mission capabilities, including orbits outside of the ecliptic plane [1–3], statites that "hover" in a fixed location [4], and interstellar travel [5–7]. Solar sail technology has advanced in recent years, and it is now possible to fabricate and deploy sails with areas of 10-100 m^2 (e.g., LightSail 2 [8] and NEA Scout [9]), with the likelihood that this will increase up to 7,000 m^2 or even larger in the coming years and decades (e.g., Solar Cruiser [3] and Solar Polar Imager [1, 2]). An unsolved challenge in the design of solar sails is ensuring its attitude and momentum can be controlled accurately and reliably using technology that scales up to the size of these large, next generation solar sails [10].

State-of-the-art solar sail attitude control methods can be sorted into three main categories: Conventional spacecraft attitude control methods (e.g., reaction wheels in the spacecraft hub [11, 12] and tip-mounted thrusters [13]), methods that control the offset between the solar sail's center of mass and center of pressure (e.g., sliding masses [13–19], shifted sails [20], billowed sails [21], variable reflectivity panels [22–25], and gimbaled ballast masses [26]), and those that use control vanes [27–31] or angled sails [32, 33].

Control methods in the first category are effective with smaller sails and relatively simple to operate, but are typically not scalable to larger solar sail designs. Methods in the second category are promising and have been incorporated into solar sail designs (e.g., Solar Cruiser uses Reflectivity Control Devices (RCDs) and an active mass translator (AMT) system [3]). However, some of them, such as sliding and gimbaled ballast masses, are difficult to scale up to larger sails, as they involve adding substantial mass to the design. Additionally, many methods within this category are incapable of generating control torques out of the plane of the sail (roll axis). Variable reflectivity panels, such as RCDs, can generate torques about the roll axis through a reflectivity gradient in the panel or a mounting offset from the normal axis of the sail, although this torque can be small in magnitude. Control methods in the third category, including control vanes, are typically capable of generating three-axis control torques, but also have limited torque capabilities due to their relatively small controllable area. For this reason, control vanes are often placed as far outwards on the sail as possible to in-

crease the torque they produce, which complicates the design of the system, specifically the storage and deployment of the sail, as well as the method of powering/controlling the vanes. Scaling up control vanes to larger solar sails is challenging, as larger control torques require vanes with larger mass and volume. A recently-proposed concept makes use of the entire solar sail as a control vane, where piezoelectric actuators are used to bend flexible booms and cause the sail to deflect, thus inducing a control torque through an imbalance in SRP [32, 33]. This technique has great potential in generating larger torques, as the entire sail is used an actuator; however, the use of piezoelectric actuation of the booms severely limits the deflections and yields small control torques.

The idea of using the entire solar sail as a control vane inspired the Cable-Actuated Bio-inspired Lightweight Elastic Solar Sail (CABLESSail) concept proposed in this paper. CABLESSail leverages lightweight cable-driven actuation to achieve large, controllable elastic bending and torsional deformations in the booms of a solar sail that mimic the motion of an elephant's trunk or a starfish's arms. These large cable-driven boom deformations, which are actuated using winches located near the solar sail's center of mass, will modulate the shape of the entire sail to act as a "control vane" and create an imbalance of SRP to induce control torques in all three solar sail axes. This actuation method scales well with an increase in solar sail size, as cables can transmit forces over kilometers in length from a lightweight and small stowed volume.

This paper highlights early work on the CABLESSail concept, focusing on 1) an initial conceptual design with preliminary analysis of the actuation requirements and magnitude of attitude control torques generated; 2) initial dynamic simulation development efforts to capture CABLESSail's structural dynamics and provide an environment in which to test the concept; 3) early prototyping results demonstrating the real-world feasibility of the proposed actuation mechanisms; and 4) plans for the control and estimation algorithms to be used to reliably actuate the cable-actuated mechanisms.

The remainder of this paper proceeds as follows. Section 2 provides a detailed overview of the CABLESSail concept and preliminary aspects of its design. Section 3 presents initial development of a CABLESSail dynamic simulation. Early prototyping results are highlighted in Section 4, followed by a discussion on CABLESSail's control and estimation challenges in Section 5. Concluding remarks are provided in Section 6.
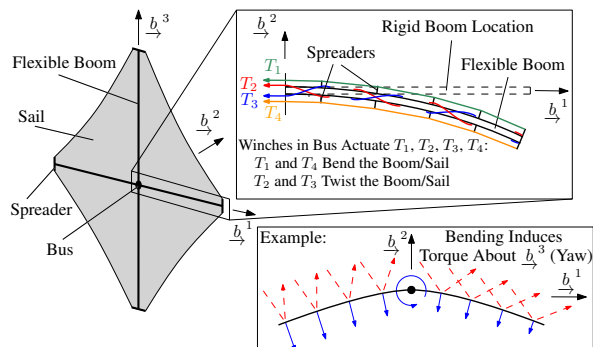
Figure 1: Schematic of the CABLESSail concept.

2. CABLESSail Concept Overview

This section presents an overview of the CABLES-Sail concept, followed by design options under consideration, and preliminary design evaluations using static simulations.

2.1. Concept of Operations

The CABLESSail concept is centered around the incorporation of cables/tendons routed throughout the booms of a solar sail, as shown in Figure 1. The cables are routed such that they pass through eyelets that are a distance from the boom's neutral axis, and thus, as the tension in the cable is increased and its length is reduced, bending or twisting of the boom is induced. Due to the unilateral force transmission of cables, a single cable provides bending or twisting actuation in a single direction (e.g., bending in the positive $\underrightarrow{b}^2$ direction shown in Figure 1, but not in the negative $\underrightarrow{b}^2$ direction). Bending is specifically achieved by routing the cable in a relatively straight line on one side of the boom, while twisting requires the cables to be routed helically about the boom. This type of cable-actuation mechanism is inspired by work in the area of bio-inspired cable-driven continuum robotics (also known as soft robotics) with applications ranging from surgical tasks [34] to ground-based locomotion [35, 36], and the manipulation of relatively small objects [36, 37].

The concept of operations in which CABLESSail induces attitude control through shape modulation is depicted in Figure 2. An idealized solar sail with four booms is shown in Figure 2(a), where photons are shown to bounce off the reflective sail surface with an incidence angle and transfer momentum to the sail in the form of solar radiation pressure. Figure 2(b) illustrates the effect of pulling on the appropriate cables to induce bending in the booms aligned in the $\underrightarrow{b}^1$ (pitch)
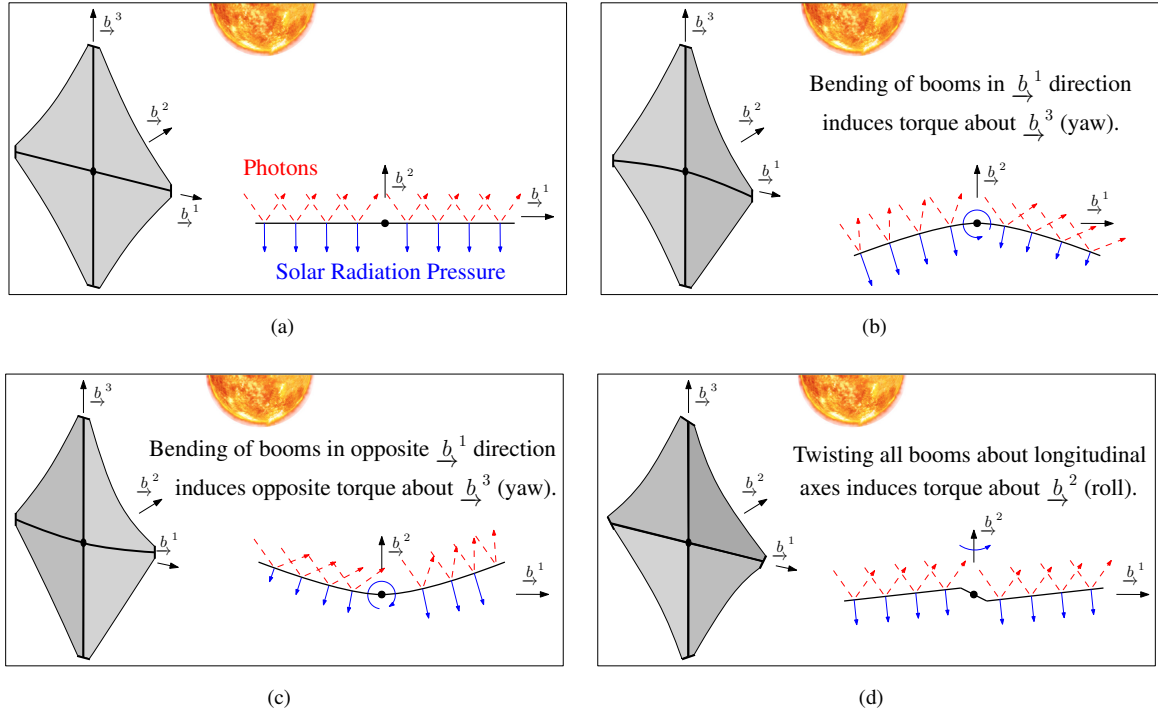
Figure 2: Schematic depicting CABLESSail's concept of operations, where the red dashed arrows denote the direction in which the photons bounce off the sail and the blue arrows denote the transfer of momentum imparted on the sail due to the photons. The undeformed sail is presented in (a). The schematic in (b) demonstrates the effect of bending the booms and sail about the yaw axis to create a smaller incidence angle on one half of the sail and a larger incidence angle on the other half of the sail, which leads to an imbalance in solar radiation pressure and a positive yaw torque. A similar effect is shown in (c), where the booms are bent in the opposite direction, resulting in a negative yaw torque. The booms are twisted in (d), which leads the sail to take on a "pinwheel" shape and induces a roll torque.

direction. This causes the shape of the sail to change such that the sun incidence angle on one side decreases, thus increasing the transfer of momentum from the photons, while the sun incidence angle of the other side of the sail increases, which decreases the transfer of momentum. This results in a net torque in the positive $\underrightarrow{b}^3$ (yaw) direction. Pulling on different cables that bend the booms in the opposite direction will induce a torque in the negative $\underrightarrow{b}^3$ direction, as shown in Figure 2(c). This approach can also be used to induce positive and negative torques in the $\underrightarrow{b}^1$ (pitch) direction by bending the booms aligned with the $\underrightarrow{b}^3$ (yaw) axis. Figure 2(d) illustrates the effect of pulling on the cables that induce a twist in all of the booms. This results in the sail taking on a pinwheel-like shape and a torque about the $\underrightarrow{b}^2$ (roll) axis is generated. Note that this pinwheel shape relies on the use of spreaders at the tips of the booms to induce a slope in the sail shape outside of the $\underrightarrow{b}^1$-$\underrightarrow{b}^3$ plane. This is a potential limitation of the CABLES-Sail design to generate roll torques, as not all solar sail designs are accommodating of tip-mounted spreaders.

2.2. Design Considerations

A central question in the design of CABLESSail is determining how to integrate the actuating cables within a deployable solar sail boom. Current work towards this is focused on assessing the possibility of integrating cables within the TRAC booms currently under development for Solar Cruiser [38], NASA Langley's ACS3 deployable booms [39], and coilable boom concepts previously developed by ATK Space Systems [40].

Another important CABLESSail design question is determining the ideal number of actuating cables. For full control over the bending and twisting of each boom in both the positive and negative directions, a total of six cables are required per boom: one cable to bend in the positive direction, one cable to bend in the negative direction, two helically-routed cables to twist in the positive direction and two helically-routed cables to twist in the negative direction. This results in a total of 24 cables actuated by motors to fully actuate all of CABLESSail's booms, which will require substantial mass and volume, while also introducing a large amount of system complexity. Fortunately, attitude control torques can be gen-

3

erated without requiring all booms to be fully actuated. For example, pitch and yaw torques can be generated by only bending one of the booms, rather than two, albeit with a smaller torque magnitude. This can reduce the need for two "boom-bending" cables in each boom down to one. The downside of this is a reduction in actuation redundancy, which will make the system susceptible to failures in any single actuating cable. A trade study is currently being conducted to quantify the trade-offs between actuator size, weight, and power (SWaP), attitude control torque magnitude, and actuation redundancy to provide guidelines on this design choice.

2.3. Preliminary Design and Static Simulation Tests

A preliminary CABLESSail design is developed for a Solar Cruiser-class sail focusing on the use of cable actuation to induce bending of the booms. For this initial design and analysis, tubular cross-section booms are considered that have a similar carbon fiber material and second moment of area to the proposed Solar Cruiser TRAC booms. Disks placed along the length of the booms are designed to route the cables 7.5 cm from the neutral axis of the booms. The booms are discretized into elements and their deformation as a function of the tension applied to the cables is computed using the tendon-driven continuum robot static modeling code developed by the University of Toronto [41]. The deformations of the discretized boom elements are then used to determine the boundary conditions of the surrounding sail quadrants. As part of this preliminary simulation, a two-dimensional representation of the sail as a flat plate between boundary conditions is used. The sail is discretized into a number of panels and the normal direction of each panel is determined to compute the local sun-incidence angle (SIA) of each panel. The idealized SRP model in [42] is used to compute the force on each sail panel, which is then used to determine the total force and moment acting on the solar sail by summing up the forces and moments acting across all sail panels.

The resulting torques generated by actuating a single cable/boom at 0 deg. SIA and 35 deg. SIA is shown in Figure 3 along with the minimum torque requirements provided by NASA to counteract the predicted disturbance torques [43]. As shown in Figure 3, the torques generated by actuating the cable exceed the Solar Cruiser disturbance torque requirements with less than a 7 mm change in length of the actuating cable. The maximum cable tension required for the largest boom deformation is 63 N. Figure 3(c) also includes a visualization of the boom deformation at the maximum cable tension, where the boom tip is displaced 0.71 m.
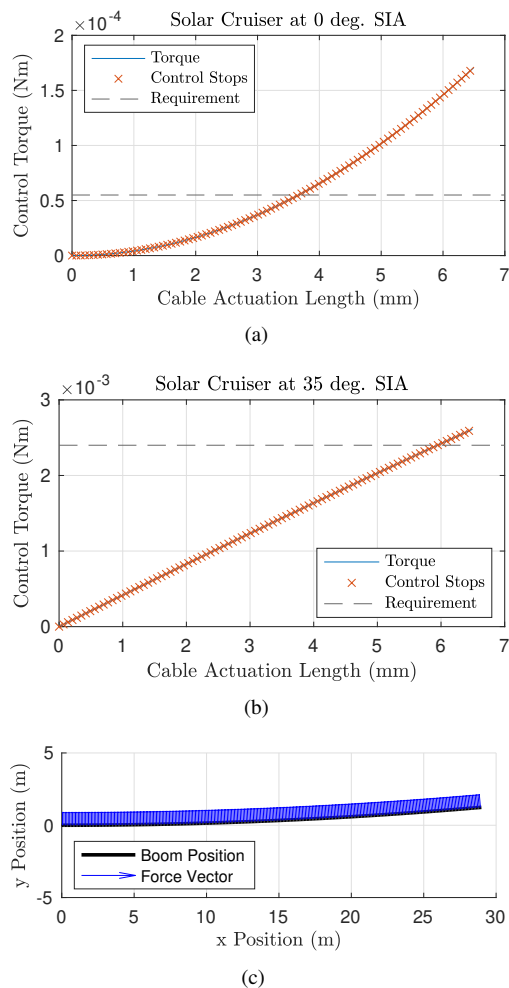
Figure 3: Results from a preliminary static simulation of the pitch and yaw control torques generated by the bending of one of CABLES-Sail's booms. The control torques generated as a function of cable actuation length at 0 deg. and 35 deg. sun-incidence angles (SIAs) are included in (a) and (b), respectively. The boom deformation at the maximum cable actuation length is shown in (c), where the SRP force vector at each sail node for 0 deg. SIA is included.

The preliminary design features eight stepper motors (Avior C62S-10N75-20) that are capable of providing more than the required 63 N of cable tension with a reasonably-sized winch drum. The motors are equipped with a mechanical brake capable of holding the winch at the desired angle when the boom is to be held in place, which reduces the power draw of the system. The total mass estimate of the CABLESSail actuation hardware is 3.1 kg, of which 1.6 kg is attributed to the motors, the actuating cables have a mass of 1 kg, and the supporting hardware (e.g., eyelets along the booms, nuts and bolts) and electronics make up the remaining 0.5 kg. In this first design iteration, the actuation mechanism is de-

signed to fit within 25 cm x 25 cm x 10 cm volume. This volume will likely be reduced in future iterations.

3. CABLESSail Dynamic Modeling

A dynamic model of the entire CABLESSail system is derived through the null-space method [44, 45], a modular dynamic modeling technique for multi-body systems with constraints. This method allows for an arbitrary number of actuating cables to be kinematically constrained to the flexible booms with arbitrary cable routings, as well as constrain the flexible booms to the bus and sail of the spacecraft. This modularity in the dynamic model and numerical simulation allows for a large design space to be tested without requiring the system's equations of motion to re-derived with each design change. An overview of the null-space method is first presented, followed by a description of how the null-space method is used to structure the CABLESSail dynamic simulation code, and initial simulation results.

3.1. Null-Space Method Overview

The equations of motion of the ith component of the system (e.g., rigid spacecraft hub, flexible boom) are derived as

$$\mathbf{M}_i(\mathbf{q}_i)\ddot{\mathbf{q}}_i + \mathbf{D}_i(\mathbf{q}_i)\dot{\mathbf{q}}_i + \mathbf{K}_i(\mathbf{q}_i)\mathbf{q}_i = \mathbf{f}_i + \mathbf{f}_{\text{non}_i}(\dot{\mathbf{q}}_i, \mathbf{q}_i), \quad (1)$$

where $\mathbf{q}_i$ contains the generalized coordinates of the ith component (e.g., position, attitude, elastic coordinates), $\mathbf{M}_i(\mathbf{q}_i)$ is the mass matrix, $\mathbf{D}_i(\mathbf{q}_i)$ is the damping matrix, $\mathbf{K}_i(\mathbf{q}_i)$ is the stiffness matrix, $\mathbf{f}_i$ contains the generalized forces and moments, and $\mathbf{f}_{\text{non}_i}(\dot{\mathbf{q}}_i, \mathbf{q}_i)$ contains nonlinear forces. The equations of motion in Eq. (1) can be derived using any methodology, such as a Langrange's equations, Kane's equations, or a Newton-Euler approach.

The kinematic constraints that must be maintained by the system's components are written out in Pfaffian form as $\boldsymbol{\Xi}(\mathbf{q})\dot{\mathbf{q}} = \mathbf{0}$, where $\mathbf{q} = \begin{bmatrix} \mathbf{q}_1^\top & \cdots & \mathbf{q}_n^\top \end{bmatrix}^\top$ and $\boldsymbol{\Xi}(\mathbf{q}) = \begin{bmatrix} \boldsymbol{\Xi}(\mathbf{q}_1) & \cdots & \boldsymbol{\Xi}(\mathbf{q}_n) \end{bmatrix}$. Examples of relevant kinematic constraints include the velocity of a point on one body matching the velocity of a point on another body, as well as the angular velocity of two bodies matching.

The constrained equations of motion are written as

$$\mathbf{M}\ddot{\mathbf{q}} + \mathbf{K}\mathbf{q} = \mathbf{f} + \mathbf{f}_{\text{non}} + \boldsymbol{\Xi}^\top \lambda, \quad (2)$$

where λ is a Lagrange multiplier that maintains the constraints specified by $\boldsymbol{\Xi}(\mathbf{q})\dot{\mathbf{q}} = \mathbf{0}$, $\mathbf{M} = \text{diag}\{\mathbf{M}_1, \dots, \mathbf{M}_n\}$, $\mathbf{D} = \text{diag}\{\mathbf{D}_1, \dots, \mathbf{D}_n\}$, $\mathbf{K} = \text{diag}\{\mathbf{K}_1, \dots, \mathbf{K}_n\}$, and the arguments of the terms in Eq. (2) are omitted for brevity.
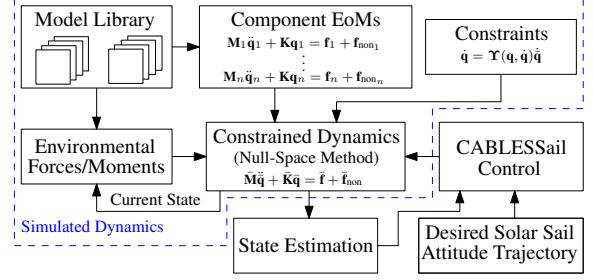
Figure 4: Block diagram of the proposed CABLESSail dynamic simulation code environment.

A set of independent coordinates $\bar{\mathbf{q}}$ is then chosen. For a system composed of rigid and flexible bodies, this is typically $\dot{\bar{\mathbf{q}}} = \begin{bmatrix} \dot{\mathbf{r}}^\top & \omega^\top & \dot{\mathbf{q}}_e^\top \end{bmatrix}^\top$, where $\dot{\mathbf{r}}$ is the velocity of the rigid body, ω is the angular velocity of the rigid body, and $\dot{\mathbf{q}}_e$ are elastic coordinate rates that describe the system's flexibility. A mapping from dependent to independent coordinates is then defined as $\dot{\mathbf{q}} = \boldsymbol{\Upsilon}\dot{\bar{\mathbf{q}}}$. Notice that $\boldsymbol{\Xi}\boldsymbol{\Upsilon} = \mathbf{0}$ (i.e., $\boldsymbol{\Xi}$ and $\boldsymbol{\Upsilon}$ are orthogonal complements) by substituting $\dot{\mathbf{q}} = \boldsymbol{\Upsilon}\dot{\bar{\mathbf{q}}}$ into the constraint $\boldsymbol{\Xi}(\mathbf{q})\dot{\mathbf{q}} = \mathbf{0}$. The independent coordinates are then substituting into the constrained equations of motion of Eq. (2) using $\dot{\mathbf{q}} = \boldsymbol{\Upsilon}\dot{\bar{\mathbf{q}}}$ and $\ddot{\mathbf{q}} = \boldsymbol{\Upsilon}\ddot{\bar{\mathbf{q}}} + \dot{\boldsymbol{\Upsilon}}\dot{\bar{\mathbf{q}}}$. The resulting equation is then premultiplied by $\boldsymbol{\Upsilon}^\top$ to yield

$$\underbrace{\boldsymbol{\Upsilon}^\top\mathbf{M}\boldsymbol{\Upsilon}}_{\bar{\mathbf{M}}}\ddot{\bar{\mathbf{q}}} + \underbrace{\boldsymbol{\Upsilon}^\top\mathbf{D}\boldsymbol{\Upsilon}}_{\bar{\mathbf{D}}}\dot{\bar{\mathbf{q}}} + \underbrace{\boldsymbol{\Upsilon}^\top\mathbf{K}\mathbf{q}}_{\bar{\mathbf{K}}\bar{\mathbf{q}}}$$
$$= \underbrace{\boldsymbol{\Upsilon}^\top\mathbf{f}}_{\bar{\mathbf{f}}} + \underbrace{\boldsymbol{\Upsilon}^\top\left(\mathbf{f}_{\text{non}} - \mathbf{M}\dot{\boldsymbol{\Upsilon}}\dot{\mathbf{q}}\right)}_{\bar{\mathbf{f}}_{\text{non}}} + \boldsymbol{\Upsilon}^\top\boldsymbol{\Xi}^\top\lambda^{\mathbf{0}}. \quad (3)$$

After the removal of the Lagrange multipliers, Eq. (3) is rewritten as

$$\bar{\mathbf{M}}\ddot{\bar{\mathbf{q}}} + \bar{\mathbf{K}}\bar{\mathbf{q}} = \bar{\mathbf{f}} + \bar{\mathbf{f}}_{\text{non}},$$

which represents the system's constrained equations of motion without Lagrange multipliers.

3.2. CABLESSail Dynamic Simulation Code Structure

Within the context of the CABLESSail simulation code, the null-space method outlined in Section 3.1 serves as a way to create code that is modular and easily amenable to design changes and the evaluation of different modeling choices. A block diagram of the proposed CABLESSail dynamic simulation code is shown in Figure 4, where its modularity and use of the null-space method are displayed. The code is structured so that a library of component equations of motion is available, which may even include different fidelity models for the
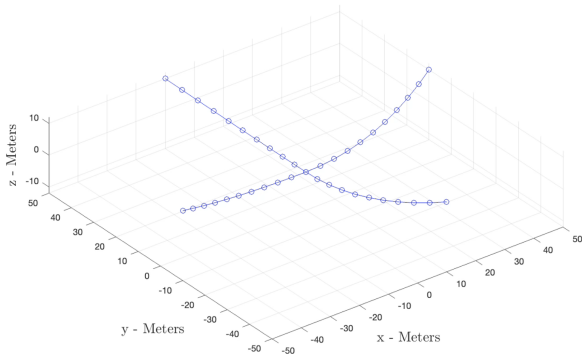
Figure 5: A screenshot of an animation from the preliminary CABLESSail dynamic simulation code.

Figure 6: A preliminary CABLESSail prototype that tests the bending motion of a single small-scale cable-actuated boom. A test with constant tension applied to the cables is shown, along with a close-up view of the winch mechanism and the 3D-printed cable-routing disks that the cables pass through.

same component. Another portion of the code is dedicated to selecting the relevant components that are to be incorporated into the simulation and also define the relevant kinematic mapping from dependent to independent coordinates $\dot{\mathbf{q}} = \Upsilon \dot{\bar{\mathbf{q}}}$. The null-space method is then used to constrain the components together, resulting in nonlinear equations of motion that can be numerically simulated in feedback with the desired stated estimation and control strategies. The versatility and modularity of the null-space method allows for drastic changes in the system configuration to be implemented in the simulation by only changing the components that are selected and defining the new mapping $\dot{\mathbf{q}} = \Upsilon \dot{\bar{\mathbf{q}}}$.

3.3. Preliminary CABLESSail Simulation Results

A preliminary version of the CABLESSail simulation code is in development, with an initial focus on modeling the elastic bending of the booms with cable-driven actuation. An animation image from this simulation is shown in Figure 5. The solar sail structure included in this simulation is representative of a CABLESSail geometry that is analogous to the dimensions of Solar Polar Imager with a free response to elastic deformations. This simulation allows for the dynamic behavior of CABLESSail's cable-actuated booms to be evaluated.

A complete three-dimensional CABLESSail simulation with a sail model inspired by [46] will be the focus of future development of this simulation code.

4. CABLESSail Prototyping

Small-scale prototyping will play an important role in the development and analysis of the CABLESSail concept. Specifically, aspects of the design that are difficult to model or simply cannot be modeled in the simulation

will be tested through the evaluation of small-scale prototypes. This will include friction between components, deployment of the booms, as well as realistic noise and delays in sensing and actuation.

The remainder of this section presents work towards an initial prototype testbed, as well as plans for future prototype fabrication and testing.

4.1. Preliminary Prototype Development

A preliminary prototype of a single CABLESSail boom with two actuating cables used to induce bending in the boom is shown in Figure 6. This prototype uses a polycarbonate boom with 3D-printed cable-routing disks along the boom. The cables are actuated by ODrive BLDC motors operated in position mode.

This preliminary prototype demonstrates the ability to generate large boom deformations using cable actuation. It also provides a framework that can be used to fabricate more advanced CABLESSail prototypes with more realistic deployable solar sail boom geometries.

4.2. Planned Future Prototypes

Additional CABLESSail prototypes will be built to guide and assess important design choices. The first set of prototypes will focus on investigating the integration of the actuating cables within deployable solar sail boom designs. Similar to the preliminary prototype discussed in Section 4.1, this will involve a single boom and test different cable routing and integration options.

A four-boom small-scale prototype will also be fabricated to test the ability to perform controlled deformation of the booms with real sensors and actuators. A motion-capture system will be used with the prototypes to provide ground-truth data of the boom deflections and assist with model validation, as well as the assessment of our proposed control and estimation algorithms.

5. CABLESSail Control and State Estimation

Successful operation of CABLESSail will rely on carefully controlled deformation of its flexible booms using actuated cables. Ensuring robustness and reliability of this actuation in the presence of CABLESSail's complex, nonlinear elastic dynamics will require an onboard autonomous feedback control strategy. Moreover, cables only transmit forces in tension and significant hardware issues can occur if a cable goes slack unintentionally. CABLESSail's feedback control strategy will need to account for these challenges, which will likely take inspiration from robust control methods developed for cable-driven robotic systems [47, 48]. Accurate knowledge of the state of the solar sail booms (e.g., its deformed shape) is required to actively control the motion of the booms. This state estimation problem is challenging, due to the nonlinear elastic deformation of the booms and vibrations in the actuating cables. Different strategies may be employed to solve this problem, ranging from fusing cable length measurements with IMU measurements [49–51] to the use of fiber optic shape sensing [52]. Feedback control and state estimation will be a central focus of future research efforts, as they are essential to performing precise, controlled deformations of the CABLESSail booms.

6. Conclusions and Future Work

The work in this paper has set the stage for the development of the CABLESSail concept. Preliminary static simulations results showed that sufficiently large attitude control torques can be generated to cancel out the disturbance torques expected for large next-generation solar sails based on the parameters of Solar Cruiser. Initial progress towards developing a modular dynamic simulation and small-scale prototypes of CABLESSail were described, along with an outline of challenges to be addressed in the areas of control and state estimation.

Future work will focus on developing CABLESSail's dynamic simulation code and assessing design options through numerical simulations and prototypes. The dynamic simulation code developed as part of this effort will be publicly released to allows for others in the community to make use of this resource.

References

[1] D. Thomas, M. Baysinger, S. Sutherlin, Q. Bean, K. Clements, K. Kobayashi, J. Garcia, L. Fabisinski, and P. Capizzo. Solar Polar Imager concept. In *ASCEND*, page 4060. 2020.

[2] K. Kobayashi, L. Johnson, H. Thomas, S. McIntosh, D. McKenzie, J. Newmark, A. Heaton, J. Carr, M. Baysingere, Q. Bean, et al. The high inclination solar mission. *arXiv preprint arXiv:2006.03111*, 2020.

[3] J. B. Pezent, R. Sood, A. Heaton, K. Miller, and L. Johnson. Preliminary trajectory design for NASA's Solar Cruiser: A technology demonstration mission. *Acta Astronautica*, 183:134–140, 2021.

[4] R. Linares, D. Landau, D. Miller, B. Weiss, and P. Lozano. Rendezvous mission for interstellar objects using a solar sail-based statite concept. *arXiv preprint arXiv:2012.12935*, 2020.

[5] X. Zeng, K. T. Alfriend, J. Li, and S. R. Vadali. Optimal solar sail trajectory analysis for interstellar missions. *The Journal of the Astronautical Sciences*, 59(3):502–516, 2012.

[6] S. Gong and M. Macdonald. Review on solar sail technology. *Astrodynamics*, 3(2):93–125, 2019.

[7] H.-T. Tung, H. Ling, and A. Davoyan. Fast transit interstellar probe mission with extreme solar sailing. In *AIAA SciTech Forum*, page 1220, 2023.

[8] D. A. Spencer, B. Betts, J. M. Bellardo, A. Diaz, B. Plante, and J. R. Mansell. The LightSail 2 solar sailing technology demonstration. *Advances in Space Research*, 67(9):2878–2889, 2021.

[9] T. R. Lockett, J. Castillo-Rogez, L. Johnson, J. Matus, J. Lightholder, A. Marinan, and A. Few. Near-Earth Asteroid Scout flight mission. *IEEE Aerospace and Electronic Systems Magazine*, 35(3):20–29, 2020.

[10] D. A. Spencer, L. Johnson, and A. C. Long. Solar sailing technology challenges. *Aerospace Science and Technology*, 93:105276, 2019.

[11] M. Polites, J. Kalmanson, and D. Mangus. Solar sail attitude control using small reaction wheels and magnetic torquers. *Proceedings of the Institution of Mechanical Engineers, Part G: Journal of Aerospace Engineering*, 222(1):53–62, 2008.

[12] H. Gong, S. Gong, and D. Liu. Attitude dynamics and control of solar sail with multibody structure. *Advances in Space Research*, 69:609–619, 2021.

[13] B. Wie and D. Murphy. Solar-sail attitude control design for a flight validation mission. *Journal of Spacecraft and Rockets*, 44(4):809–821, 2007.

[14] A. Bolle and C. Circi. Solar sail attitude control through in-plane moving masses. *Proceedings of the Institution of Mechanical Engineers, Part G: Journal of Aerospace Engineering*, 222(1):81–94, 2008.

[15] V. Lappas, G. Mengali, A. A. Quarta, J. Gil-Fernandez, T. Schmidt, and B. Wie. Practical systems design for an Earth-magnetotail-monitoring solar sail mission. *Journal of Spacecraft and Rockets*, 46(2):381–393, 2009.

[16] D. Romagnoli and T. Oehlschlägel. High performance two degrees of freedom attitude control for solar sails. *Advances in Space Research*, 48(11):1869–1879, 2011.

[17] S. N. Adeli, V. J. Lappas, and B. Wie. A scalable bus-based attitude control system for solar sails. *Advances in Space Research*, 48(11):1836–1847, 2011.

[18] W. H. Steyn and V. Lappas. CubeSat solar sail 3-axis stabilization using panel translation and magnetic torquing. *Aerospace Science and Technology*, 15(6):476–485, 2011.

[19] H. Huang and J. Zhou. Solar sailing CubeSat attitude control method with satellite as moving mass. *Acta Astronautica*, 159: 331–341, 2019.

[20] B. Fu and F. O. Eke. Attitude control methodology for large solar sails. *Journal of Guidance, Control, and Dynamics*, 38(4): 662–670, 2015.

[21] B. Fu, E. Sperber, and F. Eke. Solar sail technology—a state of the art review. *Progress in Aerospace Sciences*, 86:1–19, 2016.

[22] R. Funase, Y. Mimasu, Y. Chishiki, Y. Shirasawa, Y. Tsuda, T. Saiki, and J. Kawaguchi. Modeling and on-orbit performance evaluation of propellant-free attitude control system for spinning solar sail via optical parameter switching. In *AAS/AIAA Astrodynamics Specialist Conference*, pages 1737–1754, 2012.

[23] A. Borggräfe, J. Heiligers, M. Ceriotti, and C. McInnes. Optical control of solar sails using distributed reflectivity. In *Spacecraft Structures Conference*, page 0833, 2014.

[24] D. C. Ullery, S. Soleymani, A. Heaton, J. Orphee, L. Johnson, R. Sood, P. Kung, and S. M. Kim. Strong solar radiation forces from anomalously reflecting metasurfaces for solar sail attitude control. *Scientific Reports*, 8(1):1–10, 2018.

[25] A. R. Davoyan, J. N. Munday, N. Tabiryan, G. A. Swartzlander, and L. Johnson. Photonic materials for interstellar solar sailing. *Optica*, 8(5):722–734, 2021.

[26] E. Sperber, B. Fu, and F. O. Eke. Large angle reorientation of a solar sail using gimballed mass control. *The Journal of the Astronautical Sciences*, 63(2):103–123, 2016.

[27] D. Lawrence and S. Piggott. Integrated trajectory and attitude control for a four-vane solar sail. In *AIAA Guidance, Navigation, and Control Conference and Exhibit*, page 6082, 2005.

[28] M. Mettler, A. Acikmese, and S. Ploen. Attitude dynamics and control of solar sails with articulated vanes. In *AIAA Guidance, Navigation, and Control Conference and Exhibit*, page 6081, 2005.

[29] M. Choi and C. J. Damaren. Structural dynamics and attitude control of a solar sail using tip vanes. *Journal of Spacecraft and Rockets*, 52(6):1665–1679, 2015.

[30] O. Eldad, E. G. Lightsey, and C. Claudel. Minimum-time attitude control of deformable solar sails with model uncertainty. *Journal of Spacecraft and Rockets*, 54(4):863–870, 2017.

[31] S. Hassanpour and C. J. Damaren. Collocated attitude and vibrations control for square solar sails with tip vanes. *Acta Astronautica*, 166:482–492, 2020.

[32] F. Zhang, G. Shengping, G. Haoran, and H. Baoyin. Solar sail attitude control using shape variation of booms. *Chinese Journal of Aeronautics*, 35(10):326–336, 2021.

[33] F. Zhang, S. Gong, and H. Baoyin. Three-axes attitude control of solar sail based on shape variation of booms. *Aerospace*, 8 (8):198, 2021.

[34] T. Kato, I. Okumura, S.-E. Song, A. J. Golby, and N. Hata. Tendon-driven continuum robot for endoscopic surgery: Preclinical development and validation of a tension propagation model. *IEEE/ASME Transactions on Mechatronics*, 20(5):2252–2263, 2014.

[35] V. Vikas, E. Cohen, R. Grassi, C. Sözer, and B. Trimmer. Design and locomotion control of a soft robot using friction manipulation and motor–tendon actuation. *IEEE Transactions on Robotics*, 32(4):949–959, 2016.

[36] D. Rus and M. T. Tolley. Design, fabrication and control of soft robots. *Nature*, 521(7553):467–475, 2015.

[37] K. Oliver-Butler, J. Till, and C. Rucker. Continuum robot stiffness under external loads and prescribed tendon displacements. *IEEE Transactions on Robotics*, 35(2):403–419, 2019.

[38] L. Nguyen, K. Medina, Z. McConnel, and M. S. Lake. Solar Cruiser TRAC boom development. In *AIAA SciTech Forum*, page 1507, 2023.

[39] W. K. Wilkie, J. M. Fernandez, O. R. Stohlman, N. R. Schneider, G. D. Dean, J. H. Kang, J. E. Warren, S. M. Cook, P. L. Brown, T. C. Denkins, S. D. Horner, E. D. Tapio, M. Straubel, M. Richter, and J. Heiligers. Overview of the NASA advanced composite solar sail system (ACS3) technology demonstration project. In *AIAA Scitech Forum*, page 1260, 2021.

[40] Florio Dalla Vedova and Pierre Morin. Survey of available boom technologies, the related TRL2 (and 3) and when will we reach our solar sails missions objectives. In *4th International Symposium on Solar Sailing (ISSS)*, pages 17–20, 2017.

[41] P. Rao, Q. Peyron, S. Lilge, and J. Burgner-Kahrs. How to model tendon-driven continuum robots and benchmark modelling performance. *Frontiers in Robotics and AI*, 7:630245, 2021.

[42] Bong Wie. Solar sail attitude control and dynamics, part 1. *Journal of Guidance, Control, and Dynamics*, 27(4):526–535, 2004.

[43] Space Technology Research Grants Program, Early Career Faculty Appendix B1, February 2022.

[44] O. A. Bauchau. *Flexible Multibody Dynamics*. Springer, Dordrecht, Netherlands, 2011.

[45] R. J. Caverly and J. R. Forbes. Dynamic modeling, trajectory optimization, and control of a flexible kiteplane. *IEEE Transactions on Control Systems Technology*, 25(4):1297–1306, 2016.

[46] L. Rios-Reyes. *Solar Sails: Modeling, Estimation, and Trajectory Conrol*. PhD thesis, University of Michigan, Ann Arbor, MI, 2006.

[47] R. J. Caverly and J. R. Forbes. Flexible cable-driven parallel manipulator control: Maintaining positive cable tensions. *IEEE Transactions on Control Systems Technology*, 26(5):1874–1883, 2018.

[48] H. A. Godbole, R. J. Caverly, and J. R. Forbes. Dynamic modeling and adaptive control of flexible cable-driven parallel robots. *Journal of Dynamic Systems, Measurement, and Control*, 141 (10):101002–18, 2019.

[49] V. L. Nguyen and R. J. Caverly. Cable-driven parallel robot pose estimation using extended Kalman filtering with inertial payload measurements. *IEEE Robotics and Automation Letters*, 6(2):3615–3622, 2021.

[50] S. Patel, V. L. Nguyen, and R. J. Caverly. Forward kinematics of a cable-driven parallel robot with pose estimation error covariance bounds. *Mechanism and Machine Theory*, 183:105231, 2023.

[51] N. Puri and R. J. Caverly. Coupled least-squares forward kinematics and extended Kalman filtering for the pose estimation of a cable-driven parallel robot. *International Journal of Mechanisms and Robotic Systems*, 5(3):270–289, 2023.

[52] E. M. Lally, M. Reaves, E. Horrell, S. Klute, and M. E. Froggatt. Fiber optic shape sensing for monitoring of flexible structures. In *Sensors and Smart Structures Technologies for Civil, Mechanical, and Aerospace Systems*, volume 8345, pages 831–839, 2012.